



LAWRENCE  
LIVERMORE  
NATIONAL  
LABORATORY

# Characterization of laser-induced plasmas associated with energetic laser cleaning of metal particles on fused silica surfaces

M. J. Matthews, C. D. Harris, N. Shen, A. M. Rubenchik, S. G. Demos

October 27, 2015

Optics Letters

## **Disclaimer**

---

This document was prepared as an account of work sponsored by an agency of the United States government. Neither the United States government nor Lawrence Livermore National Security, LLC, nor any of their employees makes any warranty, expressed or implied, or assumes any legal liability or responsibility for the accuracy, completeness, or usefulness of any information, apparatus, product, or process disclosed, or represents that its use would not infringe privately owned rights. Reference herein to any specific commercial product, process, or service by trade name, trademark, manufacturer, or otherwise does not necessarily constitute or imply its endorsement, recommendation, or favoring by the United States government or Lawrence Livermore National Security, LLC. The views and opinions of authors expressed herein do not necessarily state or reflect those of the United States government or Lawrence Livermore National Security, LLC, and shall not be used for advertising or product endorsement purposes.

# Characterization of laser-induced plasmas associated with energetic laser cleaning of metal particles on fused silica surfaces

CANDACE D. HARRIS<sup>2</sup>, NAN SHEN<sup>1</sup>, ALEXANDER M. RUBENCHIK<sup>1</sup>, STAVROS G. DEMOS<sup>1</sup> AND MANYALIBO J. MATTHEWS<sup>1,\*</sup>

<sup>1</sup>Lawrence Livermore National Laboratory, 7000 East Avenue, Livermore, CA, 94550 USA

<sup>2</sup>Currently at the Department of Physics, Florida Agriculture and Mechanical University, Tallahassee, FL, 32310, USA

\*Corresponding author: [ibo@llnl.gov](mailto:ibo@llnl.gov)

Received XX Month XXXX; revised XX Month, XXXX; accepted XX Month XXXX; posted XX Month XXXX (Doc. ID XXXXX); published XX Month XXXX

**Time-resolved plasma emission spectroscopy was used to characterize the energy coupling and temperature rise associated with single, 10-ns pulsed laser ablation of metallic particles bound to transparent substrates. Plasma associated with Fe(I) emission lines originating from steel microspheres was observed to cool from >24,000 K to ~15,000 K over ~220 ns as  $\tau^{-0.28}$ , consistent with radiative losses and adiabatic gas expansion of a relatively free plasma. Simultaneous emission lines from Si(II) associated with the plasma etching of the SiO<sub>2</sub> substrate were observed yielding higher plasma temperatures, ~35,000 K, relative to the Fe(I) plasma. The difference in species temperatures is consistent with plasma confinement at the microsphere-substrate interface as the particle is ejected, and is directly visualized using pump-probe shadowgraphy as a function of pulsed laser energy.**

**OCIS codes:** (140.3440) Lasers-induced breakdown; (140.3540) Lasers, Q-Switched; (160.6030) Silica; (300.6365) Spectroscopy, laser-induced breakdown; (140.3330) Laser Damage.

<http://dx.doi.org/10.1364/OL.99.099999>

Research in the area of surface laser cleaning [1] of particulate contamination of microelectronics [2] nuclear and plasma reactors [3,4] is driven by the need to quantify performance limitations. For example, particulate contamination on high power laser optics generated through optical processing and handling can lead to damage initiation and local fracture that, if left uncorrected, can limit optic lifetime in a pulsed laser system after a few successive shots [5-7]. Surface pitting from particle ejection has been studied in a variety of configurations [8,9]. At high enough plasma temperatures and pressures a cross-over in behavior is observed whereby the surface modification and mechanical failure at the particle-substrate interface can be observed [10,11]. Therefore, characterization of the plasma produced during laser ablation of metal particles on optics could serve as an important tool in understanding contaminant-mediated, laser-induced surface

pitting. Generally, plasma characteristics depend on laser intensity, wavelength, and pulse duration, as well as on the physical and chemical characteristics of target material, and the surrounding atmosphere [12]. Because the charged ions and electrons can interact directly with the solid material and possibly cause etching, it is useful to derive both electron temperature and to evaluate the electron density through analysis of the Stark broadening effects. While extensive literature exists on plasma spectroscopy of monolithic solids, few studies exist involving single event plasma generation involving particulates on optic surfaces exposed to energetic laser pulses.

The aim of this work is to use time-resolved emission spectroscopy to probe the early phase of the plasma formation associated with fused silica surface-bound metal particles. The plasma temperature ( $T_e$ ) and electron number density ( $N_e$ ) were measured at laser intensities between ~4 to 25 GW/cm<sup>2</sup>. We show that Fe(I)-derived temperatures scale approximately linearly with laser energy and range from 15,000 to 25,000 K, while temperatures associated with Si(II) emission from substrate etching appear ~2x higher. This suggests that the plasma may be confined between the optic and the particle, leading to more effective heating than would be anticipated through monolithic plasma measurements. It is further shown that the contribution to the plasma from the optical substrate and contaminant evolves over time, yielding more substrate ions at later times. The insights gained from the analysis presented here can ultimately be used to understand better the debris mediated surface modification and to advance the understanding of laser-matter coupling relevant to debris-induced laser damage. Furthermore, although our study involves nanosecond pulsed laser-material interaction, our methods should provide guidance to a wider audience, for example ultrafast laser interaction with contaminant particles [13].

A standard spectroscopy system was used [14]. Experiments were carried out using a Q-switched, pulsed Nd:YAG laser operating at a wavelength of 1064 nm, 10 ns (FWHM) pulses that were focused by a lens with  $f = 100$  mm that gave a ~100  $\mu\text{m}$   $1/e^2$  diameter spot with up to 252 J/cm<sup>2</sup> per pulse (25.2 GW/cm<sup>2</sup> average intensity) at the exit surface of the sample. The sample was prepared by dispersing 316L stainless steel (SS316L) microspheres 30  $\mu\text{m}$  in diameter onto the exit surface (relative to laser beam propagation) of a polished and lightly HF etched UV-grade Corning 7980 fused silica window. The size of the metal particles was chosen as a near upper limit for Van der Waals

binding under practical handling conditions [1]. A CCD camera was used to monitor particles on the substrate before and after laser irradiation. The laser-induced plasma emission was collected by an objective lens (10x/0.28NA Mitutoyo M Plan APO) oriented at 90 degrees relative to the beam path and then coupled into the end of a 0.22NA 19-bundle optical fiber and guided to the entrance slit of a 0.27 m Czerny–Turner spectrometer (SPEX 270M). A 1024x1024 pixel time-gated intensified CCD was used to capture emission spectra with an average spectral resolution of 0.04 nm using a 1200 gr/mm diffraction grating for high spectral resolution. Gating the ICCD and varying the delay time allowed for the emission spectra to be temporally resolved. The gate width was varied between 10 and 100 ns. The intensities we used are well below the air optical breakdown which is about 100 GW/cm<sup>2</sup> for 1 μm light [15]. Hence, the observed plasma is generated due to the ablation and laser heating of metal and substrate. Two strong Fe(I) emission lines and one Si(II) emission line (substrate) over the spectral range 400–440 nm were used to evaluate plasma temperature and electron number density.

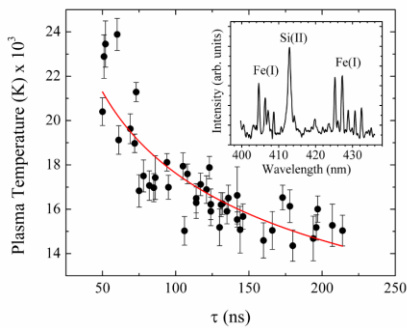


**Fig. 1.** Plasma temperature as a function of gate delay for a 316L steel particle on SiO<sub>2</sub> substrate irradiated with single 1064 nm, ~10 GW/cm<sup>2</sup> laser pulse. The inset shows a typical plasma spectrum used to derive plasma temperature from Fe(I) and Si(II) species.

We first examined the temporal dependence of the plasma temperature associated with SS316L micro-particle ejection from the fused silica surface as plotted in Fig. 1. The inset of Fig. 1 shows a typical plasma emission spectrum from irradiated SS316L particles. Several emission peaks from Fe(I) around 407 and 430 nm are observed, along with a strong Si(II) emission at ~413 nm. We chose the line-to-continuum (LTC) method and the Stark broadening effect in order to assess the plasma temperature and electron number density, respectively, over a relatively limited spectral range in which multiple species of interest were present. Here we assume that our plasma is at local thermodynamic equilibrium (LTE) where  $T_{\text{exc}} \approx T_e$  [16]. To verify that our plasma was in LTE we estimated  $T_{\text{exc}}$  using the Boltzmann two line method for emission lines Fe(I) at 407.1 nm and 427.1 nm. Both methods agreed with LTE criterion with  $T_e$  differing from  $T_{\text{exc}}$  by ~900 K.

Although the vast majority of plasma studies of laser-ablated metals are performed over micro- to milliseconds for applications such as pulsed laser machining [17,18], we are interested in the nanosecond timescale over which the plasma and particle may interact. Assuming a ~0.7 reflection loss, typical for 1 μm reflection from stainless steel spheres [15] and all the absorbed energy is converted to particle kinetic energy, an upper limit particle velocity of ~2 km/s is obtained for a 10 GW/cm<sup>2</sup> pulse, resulting in particle moving roughly its diameter in ~15 ns. 75 individual (single shot) measurements were taken over a 50 – 215 ns range with 10 ns gating revealing temperatures near 24,000 K (2.1 eV) at short times which decays over time to ~15,000 K (~1.3 eV). Previous studies on laser ablation of FeNi alloys [19] yielded a  $\tau P$  power dependence of  $p=0.22$ , whereas in the present case  $p=0.28 \pm 0.025$ . In most cases the plasma temperature for stainless steel decreases rapidly (sometimes exponentially) at early stages of plasma expansion and

maintains a relatively constant temperature thereafter [20]. The temperature drop for an adiabatic gas cloud expansion scales as  $T \sim 1/t^{3(\gamma-1)}$  where  $\gamma$  is the gas adiabatic constant [21]. The adiabatic constant can be expressed as  $\gamma = (N+2)/N$  where  $N$  is the atomic degrees of freedom. Atomic ionization produces the multiple additional degrees of freedoms and for an ionized gas the adiabatic constant is near unity. Usually, for description of an ionized gas the  $\gamma$  values in the range 1.1-1.2 are used [21]. The value  $\gamma=1.1$  is consistent with our data. The slower rate of cooling is consistent with the behavior of a confined plasma and can be

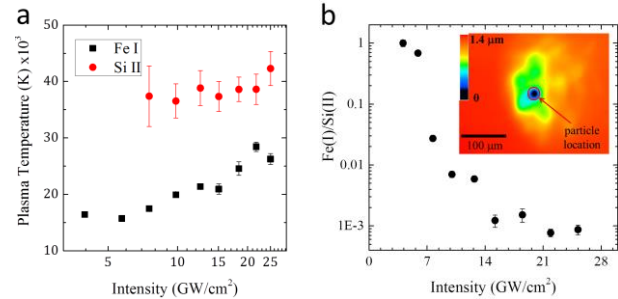


**Fig. 2.** (a) Comparison of temperatures as a function of laser intensity extracted from plasma emission lines related to the substrate (fused silica, Si(II)) and the ejected particle (SS316L, Fe(I)). (b) Natural log of the Boltzmann-normalized peak intensity ratio of [Fe (I) 427.17nm]:[Si II 413.09 nm] as a function of laser intensity at a gate delay of 220 ns. The inset shows the laser confocal microscopy image of a typical pit formed on the substrate after a ~10 GW/cm<sup>2</sup> laser pulse with the circle indicating the initial particle location.

explained by the energy re-deposition from the plasma recombination. The fast decay at the early dense stage can be related to the radiative cooling because the plasma is dense. At later times, the temperature and electron density drops, the photon mean free path becomes longer than plasma size and the role of the radiative cooling becomes less dominant.

To investigate the laser energy-dependent removal of silica caused by the laser ablation of surface bound metal particles, we used the LTC method to evaluate simultaneously the temperature associated with Si(II) and Fe(I) species generated within the ~600 μm collection area of our spectral imaging system. Figure 2a shows the temperature as a function of laser intensity plotted on a log-log scale for a gate delay of 222 +/- 8 ns. The Fe ions increase from ~15,000 K at about 5 GW/cm<sup>2</sup> to ~29,000 K near 35 GW/cm<sup>2</sup>, increasing as ~580 K/GW<sup>1</sup>cm<sup>2</sup>. On the other hand, Si ion temperatures – only measurably above 10 GW/cm<sup>2</sup> due to low 413.1 nm emission line strength – appear much hotter, ranging from ~36,000 to ~40,000 K over 11 to 35 GW/cm<sup>2</sup> laser intensities with a slope approximately half that for Fe (~230 K/GW<sup>1</sup>cm<sup>2</sup>). Because the removal of Si atoms occurs over a region smaller than the diameter of the particle, the results suggest that the plasma within the gap between the ejected particle and substrate may be confined and thus driven to higher temperatures than under weakly confined conditions.

For multicomponent plasma produced at an interface over several nanoseconds, one might expect that the temperature derived from each ionized species to be similar. In the present case, however, the specific geometry (metal sphere in contact with a flat, transparent surface) will significantly affect the energy partitioning. In particular, when laser light irradiates the metal surface after passing through the silica interface, Fe atoms are ejected through evaporation over all of the cross sectional area of the particle. In contrast, Si atoms are emitted only from a small contact region, where the Si-rich plasma is confined and can therefore be heated to higher temperatures. Thus the Fe-derived temperatures can appear lower due to the weaker confinement of the Fe plasma along the curved surface away from the contact area.

The simultaneous observation of Si and Fe emission spectra allows us to estimate the relative ion concentration. Figure 2b shows the peak intensity ratio  $\text{Fe(I)}/\text{Si(II)}$  as a function of laser intensity, after normalizing by the Boltzmann factor,  $\exp(-E/kT)$  to correct (to first order) for differences in excited state populations of the two species.  $\text{Fe(I)}/\text{Si(II)}$  decreases with increasing intensity as Si atom production and energy coupling are increased. It is well-known that at low enough laser fluence ( $<0.1 \text{ J/cm}^2$ ,  $<10 \text{ MW/cm}^2$ ), attached particles may be “dry” laser cleaned from surfaces with negligible surface damage [15]. However, it is natural that at fluences sufficient to generate plasma from attached metal particles, some energy may couple into the substrate surface causing damage. The inset of Fig. 2b displays the pit morphology (measured using laser-scanning confocal microscopy) created from a stainless steel particle on fused silica substrate irradiated by a  $\sim 10 \text{ GW/cm}^2$  pulses. This pitting was not observed on substrate without particle at the same laser intensity. We note that the profiles are smooth, in contrast to more typical, exit surface laser-induced damage which tends to display significant fracture [22,23]. While smooth pitting can be created through thermally-induced glass relaxation mechanisms leading to densification [24], our experiments confirmed that Si atomic species are also present in the laser-generated plasma, indicating vaporization and ionization of material by the hot plasma as the root cause of pitting at high fluences ( $>0.1 \text{ J/cm}^2$ ,  $10 \text{ MW/cm}^2$ ). As shown in the Fig. 2b inset, the increase in atomic Si production at high intensities ( $\sim 10 \text{ GW/cm}^2$ ) can be correlated with surface pitting which is only observed with the presence of SS particle. We therefore argue that this pitting is due to plasma etching as opposed to direct laser absorption and heating of  $\text{SiO}_2$ .

Figure 3 shows two pairs of images captured using a time-resolved microscope system described in detail elsewhere [25]. In brief, starting from the same pump laser and experimental arrangement utilized in this work, the microscope system was positioned orthogonal to the laser beam propagation direction to enable side view imaging of the sample’s surface (vertical to the surface of the substrate). The strobe light back-illumination was provided by 532 nm, 4.5 ns (FWHM) pulses from a frequency-doubled Nd:YAG probe laser. The temporal delay of the probe pulses with respect to the pump pulse was adjustable, thus allowing capturing images of the ejected particles in-flight at predetermined delays after exposure to the pump pulse. The images presented as case examples in the inset show the particle attached on the exit surface of the substrate before (right; a1, b1) and 10.5  $\mu\text{s}$  after (left; a2, b2) exposure to the pump pulse, respectively. Consequently, the image component generated by the probe laser light is at a specific delay (capturing the transient location of the particle) while the superimposed image component of the plasma is integrated in time.

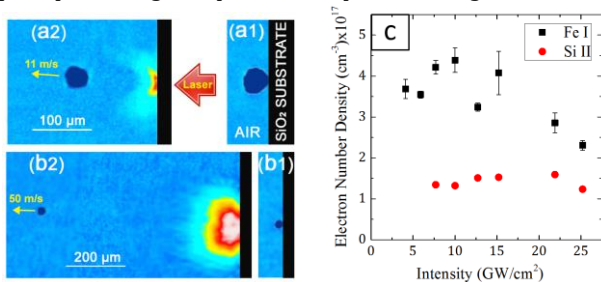


**Fig. 3.** Shadowgraphs of particle trajectories and integrated plasma emission from a  $\sim 4.1 \text{ GW/cm}^2$  pulse (a1: before, a2: after) and a  $\sim 10 \text{ GW/cm}^2$  pulse (b1: before, b2: after). Electron number density for Fe and Si as a function of laser intensity (c).

The first pair of images shows a 36- $\mu\text{m}$  diameter particle (Fig. 3a1) before and (Fig. 3a2) at 10.5  $\mu\text{s}$  delay after a single shot laser exposure to about  $4.1 \text{ GW/cm}^2$ , respectively. The distance traveled during this time is about 115  $\mu\text{m}$ , corresponding to a speed of the particle of about 11 m/s. The second pair of images shows a 25  $\mu\text{m}$  diameter particle before (Fig. 3b1) and after exposure to about  $10 \text{ GW/cm}^2$  laser pulse (Fig. 3b2) while it travels with an estimated speed of about 50.4 m/s. The speed of the particles is dependent on both the size of the particle and the laser fluence. The underlying mechanisms of this behavior will be discussed elsewhere. However, we can observe in the present time resolved images of Fig. 3a,b micro-particle inertial effects which are characterized by particle speed and can influence the expansion of the generated plasma. For lower laser energy and larger particles, the particle partially confines the plasma near the surface for a longer period of time, and particularly at early delays when the plasma temperature is higher. This confinement is evident in the image (Fig. 3a2) where the outer boundary of the hotter region of the plasma has the shape of the slow moving particle that keeps it partially confined early after energy deposition (on the order of 100 ns). On the other hand, the plasma contour in image (Fig. 3b2) generated at higher laser fluence is closer to hemispherical which would be expected in the case of a free expansion of the plasma. This confined-free plasma transition may explain the relatively weak energy dependence observed in the  $T_{\text{Si}}$  data of Fig. 2a, since confinement effects should weaken with increasing pulse energy, slowing the rise in temperature with energy.

Because the etching potential of a plasma is influenced by both temperature (ion energy) and charged species density (dosage) [26], we evaluated the electron number density,  $N_e$ , and compare it to the material removal rate as a function of laser intensity.  $N_e$  was estimated using the Stark broadening of emission lines 427.17 nm for Fe(I) and 413.08 nm for Si(II) (See Fig. 3c). Fitting each emission line to a Lorentzian fit we then used  $\Delta\lambda_{1/2} = (2WN_e)/10^{16}$  where  $\Delta\lambda_{1/2}$  is the full width half maximum and  $W$  is the electron impact parameter [27]. To further verify that the plasma was in LTE we checked that the estimated  $N_e$  was well above the lower limit [28]. Table I displays  $N_e$  for 5.9, 7.7 and  $10 \text{ GW/cm}^2$  laser intensity, along with plasma temperature in K, and substrate ablation depth in nm. For the measurements appearing in the table, pump-probe shadowgraphy using pulsed, delayed 532 nm, 7 ns probe beams allowed us to measure particle ejection velocity (complete results to be published elsewhere), and estimate the energy partitioning plasma pressure leading to particle ejection. As discussed earlier, when laser light irradiates the metal particles after passing through the silica interface, Fe atoms are ejected through evaporation over virtually all of the cross sectional area of the particle. For this reason, we see large fluctuations for the particle electron number density as the laser-particle irradiance may not be as uniform compared to the laser-substrate irradiance. (See Fig. 3c). Furthermore, recent studies on particle-plasma interactions speculate that during the first few nanoseconds of plasma expansion one side of the particle is subjected to a greater radiant flux and may consequently undergo a faster rate of vaporization [29]. On the other hand, the ablation depths increase nonlinearly as more energy is partitioned into removing  $\text{SiO}_2$  and creating a Si-rich plasma, with a rapid increase at low energy due to efficient confinement.

**Table 1.** Electron number density and plasma temperature for Fe and Si atomic species in the plasma as a function of laser irradiance along with the final pit depth and the ejected particle kinetic energy.

Laser irradiance (GW/cm <sup>2</sup> )	Electron number Density (x10 <sup>17</sup> cm <sup>-3</sup> )		Plasma Temperature (x10 <sup>3</sup> K)		Ablation pit depth (nm)	Particle velocity (m/s)
	Fe	Si	Fe	Si		
5.9	3.55±0.08	0.31±0.01	15.7±0.2	-	513±173	35±17
7.7	4.21±0.17	0.54±0.003	17.5±0.2	37.4±0.5	1068±601	48±16
10	4.39±0.30	0.53±0.003	19.9±0.4	36.5±0.3	1270±750	68±24

In conclusion, the ejection of silica surface bound steel particles by way of energetic laser pulses is shown to be accompanied by plasma containing both Fe and Si atomic species. A higher plasma temperature was extracted from the Si species relative to that of Fe, consistent with the generation of a confined Si-rich plasma at the particle-substrate interface. Shadowgraph-based plasma imaging and ejection velocity measurements further support the physical picture of confinement over the laser intensities studied, and imply an enhancement of material removal rate and surface damage due to particle ablation. Radiation reflection and plasma confinement effects in the region between the escaping particle and the substrate will enhance the laser-plasma coupling and drive the plasma to higher temperatures and electron number densities that lead to vaporization and etching of substrate material. These results are relevant to laser-induced surface pitting associated with metal contaminants on high power laser optics [30] and provide insight into the origins of pitting dependence on pulsed laser energy.

**Funding.** This work was funded by LLNL's Laboratory Directed Research and Development Program (tracking code 14ER098) and performed under the auspices of the U.S. Department of Energy by Lawrence Livermore National Laboratory under Contract DE-AC52-07NA27344. LLNL-JRNL-678662.

## REFERENCES

1. B. Luk'yanchuk, *Laser Cleaning* (World Scientific, 2002).
2. G. Vereecke, E. Rohr and M. M. Heyns, *J. Appl. Phys.* **85**, 3837-3843 (1999).
3. A. Kumar, R. B. Bhatt, M. Afzal, J. P. Panakkal, D. J. Biswas, J. P. Nilaya and A. K. Das, *Nucl. Technol.* **182**, 242-247 (2013).
4. A. Vetry, M. N. Habib, P. Delaporte, M. Sentis, D. Grojo, C. Grisolia and S. Rosanvallon, *Appl. Surf. Sci.* **255**, 5569-5573 (2009).
5. S. Palmier, S. Garcia and J. L. Rullier, *Opt. Eng.* **47**, 0842031-0842037 (2008).
6. J. Honig, M. A. Norton, W. G. Hollingsworth, E. E. Donohue and M. A. Johnson, *Proc. SPIE* **5647**, 129-135 (2005).
7. F. Y. Genin, M. D. Feit, M. R. Kozlowski, A. M. Rubenchik, A. Salleo and J. Yoshiyama, *Appl. Opt.* **39**, 3654-3663 (2000).
8. M. J. Matthews, N. Shen, J. Honig, J. D. Bude and A. M. Rubenchik, *J. Opt. Soc. Am. B* **30**, 3233-3242 (2013).
9. D. Grojo, P. Delaporte, M. Sentis, O. H. Pakarinen and A. S. Foster, *Appl. Phys. Lett.* **92**, 033108-033111 (2008).
10. N. Shen, J. D. Bude and C. W. Carr, *Opt. Express* **22**, 3393-3404 (2014).
11. S. Palmier, J. L. Rullier, J. Capoulade and J. Y. Natoli, *Appl. Opt.* **47**, 1164-1170 (2008).
12. S. Zhang, X. Wang, M. He, Y. Jiang, V. W. Hang and B. Huang, *Spectrochim Acta B* **97**, 13-33 (2014).
13. Komolov, V. L., V. E. Gruzdev, S. G. Przhibelskii and D. S. Smirnov *Opt. Eng.* **51**, 121816-121816 (2012).
14. H. C. Liu, X. L. Mao, J. H. Yoo and R. E. Russo, *Spectrochim Acta B* **54**, 1607-1624 (1999). G. G. Gladush and I. Smurov, *Physics of Laser Materials Processing* (Springer-Verlag, 2011).
15. G. G. Gladush and I. Smurov, *Physics of Laser Materials Processing* (Springer-Verlag, 2011).
16. G. J. Bastiaans and R. A. Mangold, *Spectrochim. Acta B* **40**, 885-892 (1985).

17. R. E. Russo, A. A. Bol'shakov, J. H. Yoo and J. J. Gonzalez, *Proc. SPIE* **8243**, 82430A-82430A-7 (2012).
18. G. Sarri, K. L. Lancaster, R. Trines, E. L. Clark, S. Hassan, J. Jiang, N. Kageiwa, N. Lopes, R. Ramis, A. Rehman, X. Ribeyre, C. Russo, R. H. H. Scott, T. Tanimoto, M. Temporal, M. Borghesi, J. R. Davies, Z. Najmudin, K. A. Tanaka, M. Tatarakis and P. A. Norreys, *Phys. Plasmas* **17**, 113303 (2010).
19. J. A. Aguilera and C. Aragon, *Spectrochim Acta B* **63**, 784-792 (2008).
20. H. Y. Moon, B. W. Smith, and N. Omenetto, *Chemical Physics* **398**, 221-227 (2012).
21. Ya. B. Zeldovich and Yu. P. Raizer, *Physics of shock waves and high-temperature hydrodynamic phenomena* (Dover, 2002).
22. M. J. Matthews, C. W. Carr, H. A. Bechtel and R. N. Raman, *Appl. Phys. Lett.* **99**, 151109 (2011).
23. J. Wong, J. L. Ferriera, E. F. Lindsey, D. L. Haupt, I. D. Hutcheon and J. H. Kinney, *J. Non-cryst. Sol.* **352**, 255-272 (2006).
24. Y. F. Lu, W. D. Song, K. D. Ye, M. H. Hong, D. M. Liu, D. S. H. Chan and T. S. Low, *Appl. Surf. Sci.* **120**, 317-322 (1997).
25. R. N. Raman, R. A. Negres and S. G. Demos, *Opt. Eng.* **50**, 013602 (2011).
26. Y. F. Lu, W. D. Song, K. D. Ye, Y. P. Lee, D. S. H. Chan and T. S. Low, *Jpn. J. Appl. Phys.* **2** **36**, L1304-L1306 (1997).
27. H. R. Griem, *Spectral Line Broadening by Plasmas* (Academic Press, 1974).
28. X. Z. Zeng, X. L. Mao, S. S. Mao, J. H. Yoo, R. Greif and R. E. Russo, *J. of Appl. Phys.* **95**, 816-822 (2004).
29. J. E. Carranza and D. W. Hahn, *Anal. Chem.* **74**, 5450-5454 (2002).
30. E. Feigenbaum, S. Elhadj and M. J. Matthews, *Opt. Express* **23**, 10589-10597 (2015).

## Full title references:

1. B. Luk'yanchuk, *Laser Cleaning* (World Scientific, 2002).
2. G. Vereecke, E. Rohr and M. M. Heyns, "Laser-assisted removal of particles on silicon wafers", *J. Appl. Phys.* **85**, 3837-3843 (1999).
3. A. Kumar, R. B. Bhatt, M. Afzal, J. P. Panakkal, D. J. Biswas, J. P. Nilaya and A. K. Das, "Laser-Assisted Decontamination of Fuel Pins for Prototype Fast Breeder Reactor", *Nucl. Technol.* **182**, 242-247 (2013).
4. A. Vetry, M. N. Habib, P. Delaporte, M. Sentis, D. Grojo, C. Grisolia and S. Rosanvallon, "Experimental investigation on laser removal of carbon and tungsten particles", *Appl. Surf. Sci.* **255**, 5569-5573 (2009).
5. S. Palmier, S. Garcia and J. L. Rullier, "Method to characterize superficial particulate pollution and to evaluate its impact on optical components under a high power laser", *Opt. Eng.* **47**, 0842031-0842037 (2008).
6. J. Honig, M. A. Norton, W. G. Hollingsworth, E. E. Donohue and M. A. Johnson, "Experimental study of 351-nm and 527-nm laser-initiated surface damage on fused silica surfaces due to typical contaminants" *Proc. SPIE* **5647**, 129-135 (2005).
7. F. Y. Genin, M. D. Feit, M. R. Kozlowski, A. M. Rubenchik, A. Salleo and J. Yoshiyama, "Rear-surface laser damage on 355-nm silica optics owing to Fresnel diffraction on front-surface contamination particles" *Appl. Opt.* **39**, 3654-3663 (2000).
8. M. J. Matthews, N. Shen, J. Honig, J. D. Bude and A. M. Rubenchik, "Phase modulation and morphological evolution associated with surface bound particle ablation", *J. Opt. Soc. Am. B* **30**, 3233-3242 (2013).
9. D. Grojo, P. Delaporte, M. Sentis, O. H. Pakarinen and A. S. Foster, "The so-called dry laser cleaning governed by humidity at the nanometer scale", *Appl. Phys. Lett.* **92**, 033108-033111 (2008).
10. N. Shen, J. D. Bude and C. W. Carr, "Model laser damage precursors for high quality optical materials", *Opt. Express* **22**, 3393-3404 (2014).

11. S. Palmier, J. L. Rullier, J. Capoulade and J. Y. Natoli, "Effect of laser irradiation on silica substrate contaminated by aluminum particles", *Appl. Opt.* **47**, 1164-1170 (2008).
12. S. Zhang, X. Wang, M. He, Y. Jiang, V. W. Hang and B. Huang, "Laser-induced plasma temperature", *Spectrochim Acta B* **97**, 13-33 (2014).
13. Komolov, V. L., V. E. Gruzdev, S. G. Przhibelskii and D. S. Smirnov "Dynamics of laser-induced damage of spherical nanoparticles by high-intensity ultrashort laser pulses", *Optical Engineering* **51**, 121816-121816 (2012).
14. H. C. Liu, X. L. Mao, J. H. Yoo and R. E. Russo, "Early phase laser induced plasma diagnostics and mass removal during single-pulse laser ablation of silicon", *Spectrochim Acta B* **54**, 1607-1624 (1999).
15. G. G. Gladush and I. Smurov, *Physics of Laser Materials Processing* (Springer-Verlag, 2011).
16. G. J. Bastiaans and R. A. Mangold, "The calculation of electron density and temperature in Ar spectroscopic plasmas from continuum and line spectra", *Spectrochim. Acta B* **40**, 885-892 (1985).
17. R. E. Russo, A. A. Bol'shakov, J. H. Yoo and J. J. Gonzalez, "Laser ablation plasmas for diagnostics of structured electronic and optical materials during or after laser processing", *Proc. SPIE* **8243**, 82430A-82430A-7 (2012).
18. G. Sarri, K. L. Lancaster, R. Trines, E. L. Clark, S. Hassan, J. Jiang, N. Kageiwa, N. Lopes, R. Ramis, A. Rehman, X. Ribeyre, C. Russo, R. H. H. Scott, T. Tanimoto, M. Temporal, M. Borghesi, J. R. Davies, Z. Najmudin, K. A. Tanaka, M. Tatarakis and P. A. Norreys, "Creation of persistent, straight, 2 mm long laser driven channels in underdense plasmas", *Phys. Plasmas*, **17**, 113303 (2010).
19. J. A. Aguilera and C. Aragon, "Characterization of laser-induced plasmas by emission spectroscopy with curve-of-growth measurements. Part I: Temporal evolution of plasma parameters and self-absorption", *Spectrochim Acta B* **63**, 784-792 (2008).
20. H. Y. Moon, B. W. Smith, and N. Omenetto, "Temporal behavior of line-to-continuum ratios and ion fractions as a means of assessing thermodynamic equilibrium in laser-induced breakdown spectroscopy", *Chemical Physics* **398**, 221-227 (2012).
21. Ya.B. Zeldovich and Yu.P. Raizer, *Physics of shock waves and high-temperature hydrodynamic phenomena* (Dover, 2002).
22. M. J. Matthews, C. W. Carr, H. A. Bechtel and R. N. Raman, "Synchrotron radiation infrared microscopic study of non-bridging oxygen modes associated with laser-induced breakdown of fused silica", *Appl. Phys. Lett.* **99**, 151109 (2011).
23. J. Wong, J.L. Ferriera, E.F. Lindsey, D.L. Haupt, I.D. Hutcheon and J.H. Kinney, "Morphology and microstructure in fused silica induced by high fluence ultraviolet  $3\omega$  (355 nm) laser pulses", *J. Non-cryst Sol.* **352**, 255-272 (2006).
24. Y. F. Lu, W. D. Song, K. D. Ye, M. H. Hong, D. M. Liu, D. S. H. Chan and T. S. Low, "Removal of submicron particles from nickel-phosphorus surfaces by pulsed laser irradiation", *Appl. Surf. Sci.* **120**, 317-322 (1997).
25. R. N. Raman, R. A. Negres and S. G. Demos, "Time-resolved microscope system to image material response following localized laser energy deposition: exit surface damage in fused silica as a case example", *Opt. Eng.* **50**, 013602 (2011).
26. Y. F. Lu, W. D. Song, K. D. Ye, Y. P. Lee, D. S. H. Chan and T. S. Low, "A Cleaning Model for Removal of Particles due to Laser-Induced Thermal Expansion of Substrate Surface", *Jpn. J. Appl. Phys.* **2** **36**, L1304-L1306 (1997).
27. H. R. Griem, *Spectral Line Broadening by Plasmas* (Academic Press, 1974).
28. X. Z. Zeng, X. L. Mao, S. S. Mao, J. H. Yoo, R. Greif and R. E. Russo, "Laser-plasma interactions in fused silica cavities", *J. of Appl. Phys.* **95**, 816-822 (2004).
29. J.E. Carranza and D.W. Hahn, "Assessment of the Upper Particle Size Limit for Quantitative Analysis of Aerosols Using Laser-Induced Breakdown Spectroscopy", *Anal. Chem.* **74**, 5450-5454 (2002).
30. E. Feigenbaum, S. Elhadj and M. J. Matthews, "Light scattering from laser induced pit ensembles on high power laser optics", *Opt. Express* **23**, 10589-10597 (2015).